International Journal of Science and Research Archive
eISSN: 2582-8185
Cross Ref DOI: 10.30574/ijsra
Journal homepage: https://ijsra.net/

(RESEARCH ARTICLE)

Check for updates

3-D Static modeling of hydrocarbon reservoir: A case study of Tanko field, offshore, niger delta basin

Richard Onoakpoma Akpofure * and Ovie Benjamin Ogbe

Department of Earth Science, College of Science, Federal University of Petroleum Resources, Effurun, Delta State, Nigeria.

International Journal of Science and Research Archive, 2024, 13(02), 2859-2877

Publication history: Received on 10 November 2024; revised on 09 December 2024; accepted on 12 December 2024

Article DOI: https://doi.org/10.30574/ijsra.2024.13.2.2411

Abstract

This integrated study utilized well logs and 3-D seismic data to optimize the development of hydrocarbon potentials in Tanko field. Facies evaluation identified coarse-grained sand facies, medium-grained sand facies, fine-grained sand facies, and shale, reconstructing environments of deposition, including upper shoreface, fluvial channel, tidal channel and fill. Petrophysical evaluation of seven reservoir intervals revealed shale volume range from 8-25%, total and effective porosity from 20-25% and 16-24%, NTG from 75-92.5%, water saturation from 47-99% and permeability from 381.74-967.64mD. Porosity is classified is classified as good to excellent, and permeability is very good. Seismic interpretation revealed synthetic and antithetic faults and four horizons (A, D, F, G) were mapped on seismic data and utilized as input for reservoir modelling. Time and depth structure maps revealed that reservoir closures in the field are anticlinal and fault supported. Seismic attributes showed that the closures are associated with bright amplitude anomalies which is indicative of hydrocarbon charged sands. Structural models were generated for reservoir A, D, F and G. These models were the framework for facies and petrophysical properties distribution. Facies models were generated using sequential indicator simulation algorithm while petrophysical properties were generated using sequential gaussian simulation algorithm. The facies models were used to constrain the distribution of reservoir petrophysical properties (shale volume, effective porosity, permeability and water saturation). Based on these models, the reservoir intervals were classed as having good to very good quality, especially at the well points. Hydrocarbon volumes were calculated using both deterministic and stochastic approaches. Stock tank oil initially in place estimated using the deterministic approach was 740.90MSTB, 37.38MMSTB, 197.93MMSTB and 85.88MMSTB, while using a stochastic approach, P50 volumes were 512.25M, 41.37MM, 210.00MM and 65.04MM (P50) for prospective areas in reservoir A, D, F and G. These results showed that all reservoir intervals are economically viable, with no significant difference in the hydrocarbon volumes quantified using either of the two approaches. Hence, on the fly decisions can be made regarding production without necessarily building complex stochastic models with several realizations. This study has also demonstrated the effectiveness of 3-D static modeling technique as a tool for better understanding of spatial distribution of discrete (facies) and continuous reservoir properties (petrophysical properties), hence, has provided a framework for future prediction of reservoir performance and production behavior of reservoir A, D, F and G.

Keywords: Petrophysical; Deterministic; Algorithm; Synthetic; Antithetic; Simulation

1. Introduction

Facies refers to the characteristic appearance of a rock unit, often defined by its lithology, sedimentary structures, and fossil content. Petrophysical modelling involves creating mathematical representations of rock properties such as porosity, permeability and saturation based on various data like well logs, core samples and seismic data. It is used in oil and gas exploration to understand reservoir behavior and optimize production.

* Corresponding author: Akpofure O.R

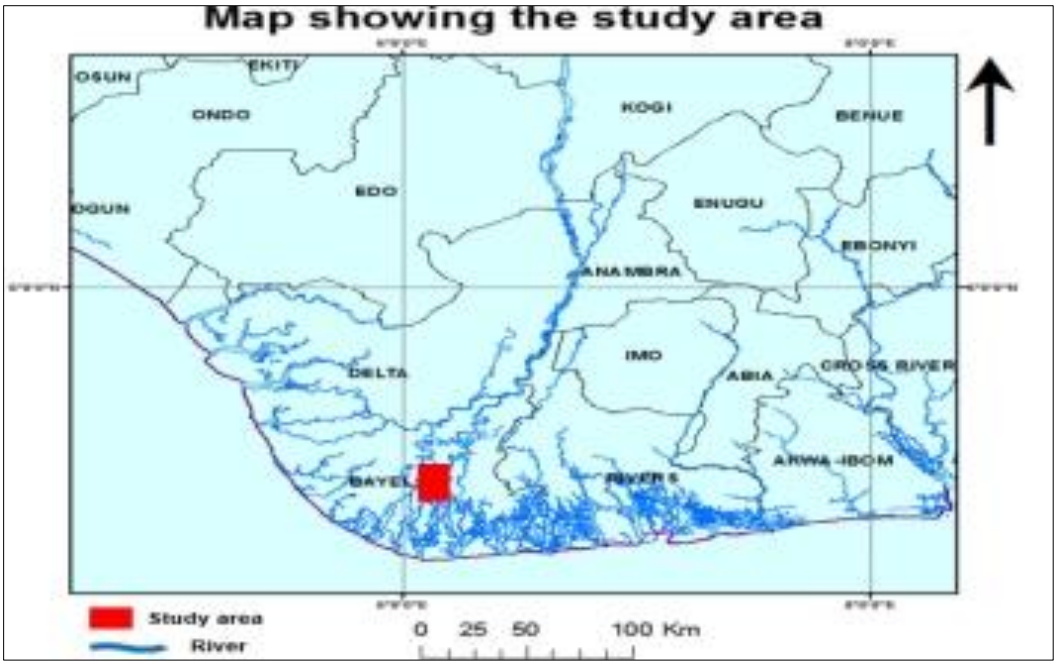

Figure 1 Base map of study area

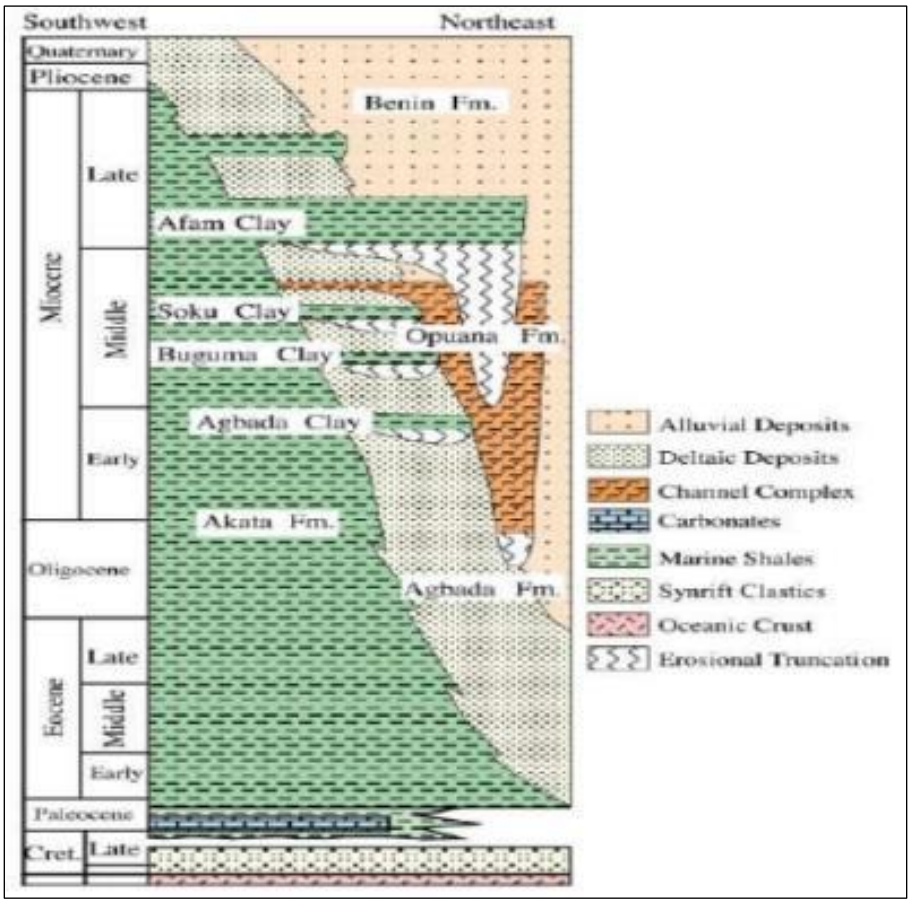

Figure 2 Three Formations of the Niger Delta shown in a stratigraphic column

The integration of facies analysis and petrophysical modelling provides a comprehensive understanding of reservoir architecture, fluid distribution and potential production yields. Facies analysis entails the detailed examination and classification of sedimentary rocks based on their depositional environment, lithological composition, and associated sedimentary structures. This research is a comprehensive investigation into the facies and petrophysical characteristics of hydrocarbon reservoirs, with a focus on enhancing exploration and production efficiency through the integration of geological observations, petrophysical analyses, and computational modeling techniques.

The location of Tanko field in Niger Delta is in the eastern region and is geo-referenced with Nigeria Mid-Belt coordinate reference system. It is an onshore field, owned and operated by Shell Petroleum Development Company (SPDC). The field is defined by its seismic data coverage and extends from latitude $4^0$35'00"N to $4^0$39'00"N and longitude $6^0$16'00"E to $6^0$20'00"E with an area of 43.84 km^2.

2. Literature Review

Reservoir modeling is a crucial step in understanding the physical behavior of hydrocarbon reservoirs. According to Adiela et al. (2017), a reservoir model represents the physical space of the reservoir as an array of discrete cells, defined by a grid that can be regular or irregular. Mathematical models used in reservoir modeling can be either deterministic or stochastic, depending on the level of uncertainty associated with the input data (Cannon, 2018). Deterministic models have a single realization, whereas stochastic models can have multiple realizations, each honoring the statistical input and range of values. Reservoir models can be categorized as map-based (two-dimensional) or grid-based (three-dimensional). Map-based models vary properties only in the x and y directions, using different mapping algorithms to distribute the outcomes. In contrast, grid-based models vary properties in all three dimensions (x, y, and z), defined by the geometry of the geological structure (Cannon, 2018).

Ovie B. Ogbe, (2021) carried out reservoir sandstone grain-size; implications for sequence stratigraphic and reservoir depositional modeling in Otovwe field, onshore Niger Delta. The grain-size distribution and the complexity of the sand-body suggests a high degree of heterogeneity of the depositional environments of clastic reservoirs. To understand the facies and depositional environments distribution of the oil-bearing sandstone reservoir in the Otovwe field, onshore Niger Delta Basin, an integrated sedimentological approach was employed. This involves the integration of well log signatures and log-probability plots of grain-size analyses of ditch-cuttings obtained from 3 wells that showed variability in the rates of oil production. The result suggests that the sediments were deposited in a fluvial environment that contains point bars of a lowstand systems tract; delta front environment that contains mouth bars and distributary channel deposits of a highstand and lowstand systems tracts, respectively; and the nearshore environment with tidal flat sediments of a transgressive systems tract.

Reservoir characterization and modeling studies have been conducted in various fields in the Niger Delta Province to understand the complexity of the reservoirs and estimate hydrocarbon reserves. Okpogo et al. (2018) carried out a study in Orok Field, Niger Delta Province, using well logs, 3-D seismic, and check-shot data. They identified four gas-bearing reservoirs with effective porosity ranging between 18 and 20% and hydrocarbon saturation between 77 and 90%. The study estimated 151 billion cu.ft and 286 billion cu.ft of gas in two of the most viable prospects.

Similarly, Oyeyemi et al. (2018) built a 3-D lithofacies and depositional model in western Niger Delta using Sequential Indicator Simulation (SIS) method. They identified three lithofacies - sand, shaly sand, and shale units - and modeled them. The study revealed a shoreline-shelf system with potential source rocks and caprocks for hydrocarbon accumulation.

Toba et al. (2018) used a reservoir modeling approach to predict reservoir performance in "AWE field", Eastern Niger Delta. They utilized seismic data, well logs, and checkshot data and distributed rock petrophysical properties and facies within a 3-D grid using a deterministic approach. The study recorded stock tank oil initially in place (STOIIP) of 156MMSTB and 127MMSTB for two reservoirs, indicating economic viability.

Aigbadon et al. (2017) carried out depositional facies studies and reservoir characterization of Usani field in the Niger delta basin. They identified channels with highly thief zones and distributed sedimentary facies. The study showed porosity ranging from 14% to 28%, permeability from 245.70 md to 454.7md, and hydrocarbon saturation from 45.50% to 78.50%.

3. Materials

The materials utilized for this research includes the following;

- Well Headers
- Log Headers
- Well logs (in ASCII)
- Well Deviation Surveys
- Checkshot Survey
- 3-D Seismic Data

Table 3.1 provides an inventory of the available dataset used for this study. The software suite employed for data visualization and interpretation is Schlumberger Petrel (version 2014.1). Petrel was chosen due to its extensive adoption and application in the exploration and production sector of the petroleum industry. Its widespread acceptance is evident in the numerous paper publications, technical presentations, and webinars that utilize Petrel. As a result, Petrel has become the industry standard for subsurface interpretation in the oil and gas sector. Its versatility and robustness make it an ideal platform for analyzing and visualizing complex subsurface data. With Petrel, the study aims to gain a deeper understanding of the reservoir's properties and behavior, ultimately leading to more informed decisions in the exploration and production process. By leveraging Petrel's capabilities, the study seeks to contribute to the advancement of knowledge in the field and align with industry best practices.

Table 1 Data inventory showing the available log dataset for this research.

Well Name	Well Header	Log Header	Well Deviation	Checkshot	GR	CALI	RES	NPHI	RHOB	SONIC
W-5	YES	YES	YES	NO	YES	YES	YES	YES	YES	YES
W-7	YES	YES	YES	NO	YES	YES	YES	YES	YES	NO
W-10	YES	YES	YES	NO	YES	YES	YES	YES	YES	YES
W-11	YES	YES	YES	YES	YES	YES	YES	YES	YES	YES

4. Methodology

4.1. Well Header

The dataset provided included well headers for all four available wells (Table 1), which contained essential information about each well. The well header data consisted of well names, geographic coordinates (Eastings and Northings), well datum reference values (Kelly Bushing, KB), and total drilled depth for each well. To ensure accuracy, the well header information was crosschecked against the log headers to detect any potential discrepancies. Once verified, the well header information was loaded into Schlumberger Petrel for further analysis.

4.2. Well Deviation

Well deviation survey data was available for all four wells (Table 3.1), providing crucial information on the exact well trajectory. This data was entered into Petrel immediately after loading the well headers. The well deviation survey file contains vital information, including the drill depth (in meters), azimuth, and inclination (dip) for each well. With this data, the true vertical depth of the well can be accurately calculated. Once the well deviation data was loaded, the wells were no longer assumed to be vertical, but instead, were represented as deviating from the vertical at different angles, reflecting their actual trajectories.

4.3. Well logs

Well logs were available for all four wells (Table 3.1). The logs available included gamma ray log (GR in gAPI unit), caliper log (CALI in metres), resistivity log (RES in Ohm.m), density log (RHOB in g/cm^3), neutron log (NPHI in m^3/m^3) and sonic log (DT in μs/ft). The well logs were provided in ASCII digital format. There were no hard copies (printed logs) provided or validation. The well logs were loaded into Petrel in ASCII format and attached to their respective templates. Afterwards, the scale of each of the log was set as follows; GR (0-150 gAPI), Caliper (6-16 inches), resistivity (0.2 to 2000

Ohm.m), neutron (0-60 m^3/m^3), density (1.65-2.65 g/cm^3) and sonic (40-240 µs/ft). The GR and CALI logs were in the same tract, NPHI and RHOB were in the same tract and with NPHI reversed for identification of gas bearing zones.

4.4. Checkshot Survey

Checkshot was available for only well W-11 (Table 3.1). The checkshot data contains depth (in metres) and two-way-time (in m/s). This data is needed for the generation of a time depth relationship for seismic well ties and conversion of surfaces from time to depth. The checkshot was loaded into Petrel and attached to the well that contains the checkshot (W-11). After loading the checkshot, it was visualized in a function window where it was plotted as depth (on the vertical axis) versus time (on the horizontal axis).

4.5. Lithology Identification and Correlation

Lithology identification was achieved with the aid of the gamma ray log, which provided a detailed profile of the subsurface geology. The sand baseline and shale baseline were determined for each well by analyzing the gamma ray log responses. The sand baseline was identified as the highest mode GR occurrence at the lower spectrum, while the shale baseline was identified as the highest mode GR occurrence at the higher spectrum. The sand/shale cutoff was then selected as the mid-point between the sand baseline and the shale baseline for each well.

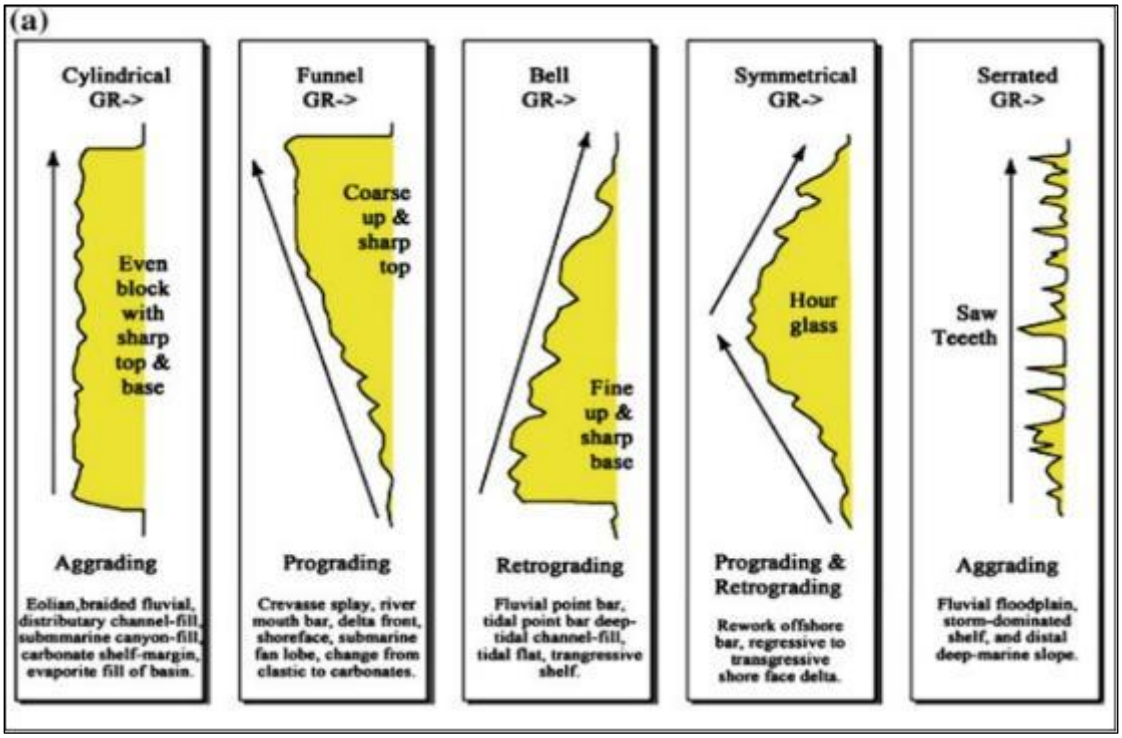

Figure 3 Gamma ray log response to stacking pattern/grain size variation model

Gamma ray values that deflected to the left of the established cutoff indicated clean sand, while deflections to the right of the cutoff indicated shales. This allowed for the identification of lithology across all wells. The lithology identification was supported by the behavior of the caliper tool and the neutron-density crossing. In sandy intervals, the caliper log was fairly straight, while in shaly intervals, the hole diameter was either too large or too small with a high degree of rugosity.

Five trends were utilized as aids for the correlation process: Cylindrical, Funnel, Bell, Symmetrical, and Serrated. Each motif represented a specific depositional pattern, allowing for the interpretation of the subsurface geology. The cylindrical log response showed an even block with a sharp top and base, indicating a consistent grain size. The funnel-shaped log motif showed a progradational pattern, with grain size increasing with decreasing depth. The bell-shaped log motif showed a decrease in grain sizes with decreasing depth, indicating a retrogradational pattern.

A symmetrical motif showed a progradational base and a retrogradational top, while a serrated log motif showed an aggradational log motif with a saw-tooth behavior (Fig. 3.2). The thickness of the shale beds also aided in reservoir

correlation, as it had a fairly consistent thickness across all wells. Before commencing the correlation exercise, the wells were arranged based on closeness to each other to recognize facies lateral geometry. The correlation exercise began from the base and progressed to the top to recognize depositional trends.

4.6. Petrophysical Evaluation

Petrophysics, as defined by Tiab and Donaldson (2004), is the scientific study of rock properties and their interactions with various fluids, including gases, liquid hydrocarbons, and aqueous solutions. In the context of petroleum studies, petrophysical properties are the characteristics of reservoir rocks that enable them to store and transmit reservoir fluids, thereby facilitating the quantitative determination of in-situ hydrocarbon reserves and the appropriate method of fluid extraction.

Four primary petrophysical parameters are crucial in defining a reservoir, namely: shale volume (VSH), effective porosity (ØT), permeability (K), and water saturation (SW). These parameters are essential in understanding the reservoir's storage capacity, fluid flow, and overall potential for hydrocarbon production.

4.6.1. Shale Volume (V_{SH})

This is the space occupied by shale or the fraction of shale (clay), present in reservoir rock (Cannon, 2017). The volume of shale is determined from mathematical correlations and gamma ray index. In mathematical equations, the volume of shale is represented as V_{SH}. The gamma ray index (GR_{index}) was first calculated in order to calculate the shale volume based on Schlumberger (1974) empirical equation as follows;

$$\mathrm{GR}_{\mathrm{index}} = \frac{GR_{log} - GR_{min}}{GR_{max} - GR_{min}} \quad \text{.....(3.1)}$$

Where;

$GR_{log} = GR\ log\ reading\ of\ formation$
$GR_{min} = GR\ sand\ baseline$
$GR_{max} = GR\ shale\ baseline$

The Larinov (1969) equation for tertiary reservoirs was utilized for calculating the shale volume as follows;

$$\mathrm{Vsh} = 0.083 \times (2^{(3.7 \times GR_{index})} - 1) \quad \text{.....(3.2)}$$

4.6.2. Total Porosity

Porosity is the fraction of the bulk volume of a material (rock) that is occupied by pores (voids). Denoted as ϕ, porosity can also be defined as the ratio of the volume of void spaces in a rock to the total volume of the rock (Cannon, 2017). Porosity is expressed in decimal or percentage and can represent the total volume of a rock occupied by empty space. Porosity can be determined using either density log, sonic or neutron-density log. It is widely accepted today that porosity determined from the density tool is most reliable amongst others (Cannon, 2018). Total porosity (Φ_T) in this study was determined using density log. The method was based on Dresser Atlas (1979) equation as follows;

$$\Phi t = \frac{\rho_{ma} - \rho_{log}}{\rho_{ma} - \rho_{fl}} \quad \text{.....(3.3)}$$

Where;

$\rho ma = density\ of\ the\ rock\ matrix\ (2.65 g/cm^2)$
$\rho log = Density\ reading\ from\ log$
$\rho fl = Density\ of\ fluid\ (water = 1 g/cm^2)$

4.6.3. Effective porosity

The effective porosity is the porosity that is responsible for flow to occur within the reservoir. Effective porosity (Φ_E) was calculated using volume of shale (Vsh) and total porosity (Φ_T) as follows (Dresser, 1979);

$$\emptyset_E = (1 - Vsh) \times \emptyset_T \quad \text{.....(3.4)}$$

Where;

$\emptyset_E = Effective\ porosity$
$\emptyset_T = Total\ Porosity$
$Vsh = Volume\ of\ shale$

4.6.4. Net to Gross

The net-to-gross ratio reduces the maximum reservoir thickness to the anticipated pay (permeable reservoir) thickness. Net-to-Gross sand is reservoir thickness less shale thickness (Cannon, 2017). This is a factor used to identify probable producing regions of a formation. To determine the clean sand content, Net to Gross was calculated as follows;

$$Net - to - gross = \frac{NH}{GH} \quad \text{.....(3.5)}$$

Where;

$NH = Net\ thickness$
$GH = Gross\ thickness$

4.6.5. Water Saturation

This is the relative extent to which the pores in rocks are filled with water. Saturation is expressed as the fraction, or percent, of the total pore volume occupied by the oil, gas, or water (Cannon, 2017). Water saturation is denoted as Sw and is expresses in percent or fraction. In this research, water saturation was calculated based on Udegbunam and Ndukwe (1988) as follows;

$$\frac{Sw=0.082}{\emptyset_T} \quad \text{.....(3.6)}$$

Where;

$Sw = Water\ saturation$
$\emptyset_T = Total\ Porosity$

4.6.6. Permeability

In fluid flow, permeability characterizes the ease with which fluids flow through a porous medium. Theoretically, permeability is the intrinsic property of a porous medium, independent of the fluids involved. Permeability is denoted as K and expressed in Darcy or millidarcy. Permeability is the measure of the ease with which a fluid flows through a rock. Owolabi et al., (1994) permeability equation which is widely used in the Niger Delta, was used in calculating the permeability for the reservoirs of interest as follows;

$$K(mD) = 307 + 26552(\emptyset^2) - (\emptyset \times S_w)^2 \quad \text{.....(3.7)}$$

4.7. Facies Determination

Volume of shale was used for determining the various facies units. The equation was entered into Petrel well calculator to generate the facies log as follows;

$$Facies = if(Vsh < 0.12.0.\ if(Vsh \geq 0.12\ And\ Vsh \leq 0.16.1.\ if(Vsh \geq 0.16\ And\ Vsh = 0.27.2.3)\ ) \quad \text{..... (3.8)}$$

4.8. Reservoir Modelling

Reservoir modeling is a comprehensive process that involves building detailed and representative models of various aspects of the reservoir. These models serve as a virtual representation of the reservoir, capturing its key characteristics and properties. The models can encompass various aspects, including:

- Structural models: Depicting the reservoir's geological framework, including fault networks, fracture systems, and stratigraphic architecture.

- Facies models: Representing the spatial distribution of different rock types and depositional environments.
- Depositional models: Reconstructing the reservoir's geological history, including sedimentary processes and paleoenvironmental conditions.
- Petrophysical models: Quantifying the reservoir's physical properties, such as:
    - Shale volume models: Estimating the proportion of shale in the reservoir.
    - Porosity models: Characterizing the reservoir's storage capacity.
    - Permeability models: Describing the reservoir's fluid flow properties.
    - Water saturation models: Defining the distribution of water within the reservoir.

These models are essential for understanding the reservoir's behavior, predicting hydrocarbon flow, and optimizing recovery strategies. By integrating data from various sources, reservoir modeling provides a robust framework for decision-making in exploration and production.

5. Results and discussion

5.1. Presentation of Results

The results for facies and petrophysical modelling of "Tanko field" are presented in Figures 4.1 to 4.30 and Tables 4.1 to 4.7 respectively.

5.1.1. Results of Facies Analysis

The results of the facies analysis are presented in Figure 4.1a, which illustrates the interpreted environment of depositions. The electrofacies recognized from the GR log motif include: Coarse-grained sands, Medium-grained sand, Fine-grained sand and Shales

These facies were used to determine the following environments of deposition:

- Upper shoreface
- Fluvial channel
- Channel fill
- Tidal channel

The reservoirs were categorized based on their depositional environments:

- Reservoir A and F: Composed of prograding parasequences (funnel-shaped) capped by aggrading parasequences (cylindrical-shaped), indicative of upper shoreface deposits overlain by fluvial channel sands.
- Reservoir B: Composed of aggrading parasequences (cylindrical-shaped), suggesting channel fill sands.
- Reservoir C, D, and E: Tidal channel sands composed of thin bedded sands showing serrations and sandwiched between thick shale beds.
- Reservoir G: Shows an aggrading parasequence (cylindrical-shaped) stacking pattern with minor serrations, indicative of channel fill sands.

Figure 4.1b presents a geologic framework for four selected reservoir intervals (A, D, F, and G), which are the focus of this study. This framework provides a detailed understanding of the reservoirs' geological structure and depositional environments, essential for building accurate reservoir models.

Table 2 Results of petrophysical evaluation for reservoir sand intervals in well W-5

Reservoir sands	Top (m)	Base (m)	Gross thickness (m)	Shale volume (%)	Net to Gross (frac.)	Total Porosity (frac.)	Effective Porosity (frac.)	Water saturation (frac.)	Permeability (mD)	Hydrocarbon saturation (frac.)	Fluid type	Fluid contact	Pay thickness (m)
Sand A	3171	3271	100	0.16	84.40	0.25	0.21	0.80	549.92	0.20	Oil and Water	OWC=3174 m	3.00
Sand B	3323	3341	18	0.09	91.00	0.26	0.24	0.56	1252.90	0.44	Oil	ODT	16.38
Sand C	3372	3383	11	0.26	74.00	0.20	0.15	0.99	530.65	0.01	Water	WUT	nil
Sand D	3418	3444	26	0.30	70.00	0.25	0.18	0.38	1149.38	0.62	Oil and Water	OWC=3441 m	23.00
Sand E	3486	3515	29	0.32	68.00	0.21	0.15	0.47	817.83	0.53	Oil and Water	OWC=3502 m	16.00
Sand F	3555	3665	110	0.22	78.00	0.22	0.18	0.56	895.69	0.44	Oil and Water	OWC=3642 m	87.00
Sand G	3763	3847	84	0.10	90.00	0.22	0.20	0.31	1220.14	0.69	Oil and Water	OWC=3835 m	72.00

OWC – oil water contact; ODT – oil down to; WUT – water up to

Table 3 Results of petrophysical evaluation for reservoir sand intervals in well W-7

Reservoir sands	Top (m)	Base (m)	Gross thickness (m)	Shale volume (%)	Net to Gross (frac.)	Total Porosity (frac.)	Effective Porosity (frac.)	Water saturation (frac.)	Permeability (mD)	Hydrocarbon saturation (frac.)	Fluid type	Fluid contact	Pay thickness (m)
Sand A	3167	3243	76	0.14	86.00	0.24	0.22	0.99	582.92	0.01	Water	WUT	Nil
Sand B	3279	3298	19	0.10	90.00	0.22	0.21	0.21	1165.34	0.79	Oil	ODT	19.00
Sand C	3318	3344	26	0.22	78.00	0.19	0.17	0.99	440.48	0.01	Water	OWC=3326 m	8.00
Sand D	3382	3407	25	0.24	76.00	0.23	0.12	0.31	1103.23	0.69	Oil	ODT	25.00
Sand E	3431	3451	20	0.31	69.00	0.22	0.20	0.24	654.80	0.76	Oil	ODT	20.00
Sand F	3496	3675	179	0.19	81.00	0.20	0.18	0.45	923.14	0.55	Oil and Water	OWC=3568 m	72.00
Sand G	3755	3858	103	0.11	89.00	0.21	0.19	0.51	1345.66	0.49	Oil and Water	OWC=3810 m	55.00

OWC – oil water contact; ODT – oil down to; WUT – water up to

Table 4 Results of petrophysical evaluation for reservoir sand intervals in well W-10

Reservoir sands	Top (m)	Base (m)	Gross thickness (m)	Shale volume (%)	Net to Gross (frac.)	Total Porosity (frac.)	Effective Porosity (frac.)	Water saturation (frac.)	Permeability (mD)	Hydrocarbon saturation (frac.)	Fluid type	Fluid contact	Pay thickness (m)
Sand A	3193	3292	99	0.21	78.70	0.25	0.20	-	-	-	-	-	-
Sand B	3340	3359	19	0.06	94.00	0.26	0.24	-	-	-	-	-	-
Sand C	3391	3401	10	0.26	74.00	0.18	0.14	-	-	-	-	-	-
Sand D	3458	3474	16	0.15	85.00	0.25	0.21	-	-	-	-	-	-
Sand E	3523	3542	19	0.15	85.00	0.23	0.20	-	-	-	-	-	-
Sand F	3580	3677	97	0.14	86.00	0.23	0.20	-	-	-	-	-	-
Sand G	3763	3869	106	0.07	93.00	0.23	0.21	0.39	1190.10	0.61	Oil and Water	OWC=3830 m	67.00

OWC – oil water contact

Table 5 Results of petrophysical evaluation for reservoir sand intervals in well W-11

Reservoir sands	Top (m)	Base (m)	Gross thickness (m)	Shale volume (%)	Net to Gross (frac.)	Total Porosity (frac.)	Effective Porosity (frac.)	Water saturation (frac.)	Permeability (mD)	Hydrocarbon saturation (frac.)	Fluid type	Fluid contact	Pay thickness (m)
Sand A	3179	3301	122	0.12	88.00	0.25	0.23	0.99	45.37	0.01	Water	WUT	nil
Sand B	3345	3356	11	0.06	94.00	0.23	0.22	0.99	307.07	0.01	Water	WUT	nil
Sand C	3387	3408	21	0.13	87.00	0.23	0.20	0.99	60.59	0.01	Water	WUT	nil
Sand D	3464	3476	12	0.25	75.00	0.21	0.16	0.89	310.87	0.11	Oil and Water	OWC=3467 m	3.00
Sand E	3500	3518	18	0.19	81.00	0.23	0.19	0.44	1165.03	0.56	Oil and Water	ODT	14.58
Sand F	3558	3705	147	0.09	91.00	0.24	0.22	0.80	446.05	0.20	Oil and Water	OWC=3609 m	51.00
Sand G	3827	3924	97	0.10	90.00	0.24	0.22	0.87	240.18	0.13	Oil and Water	OWC=3838 m	11.00

OWC – oil water contact; ODT – oil down to; WUT – water up to

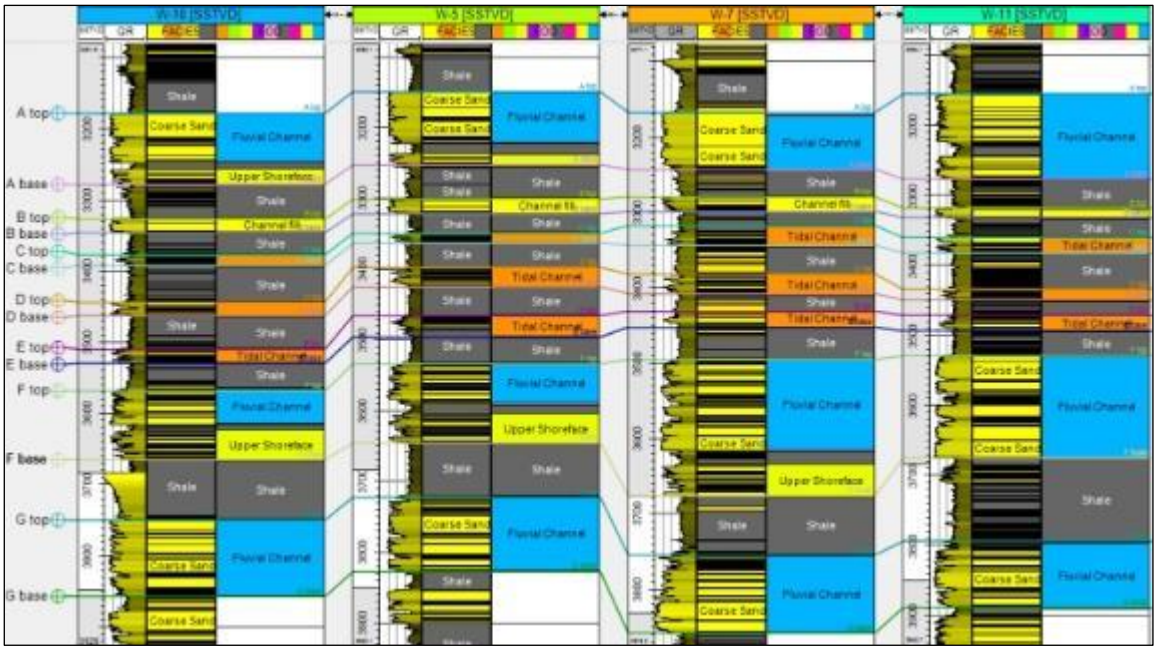

Figure 4 Facies and environment of deposition inferred for reservoir sands within the field

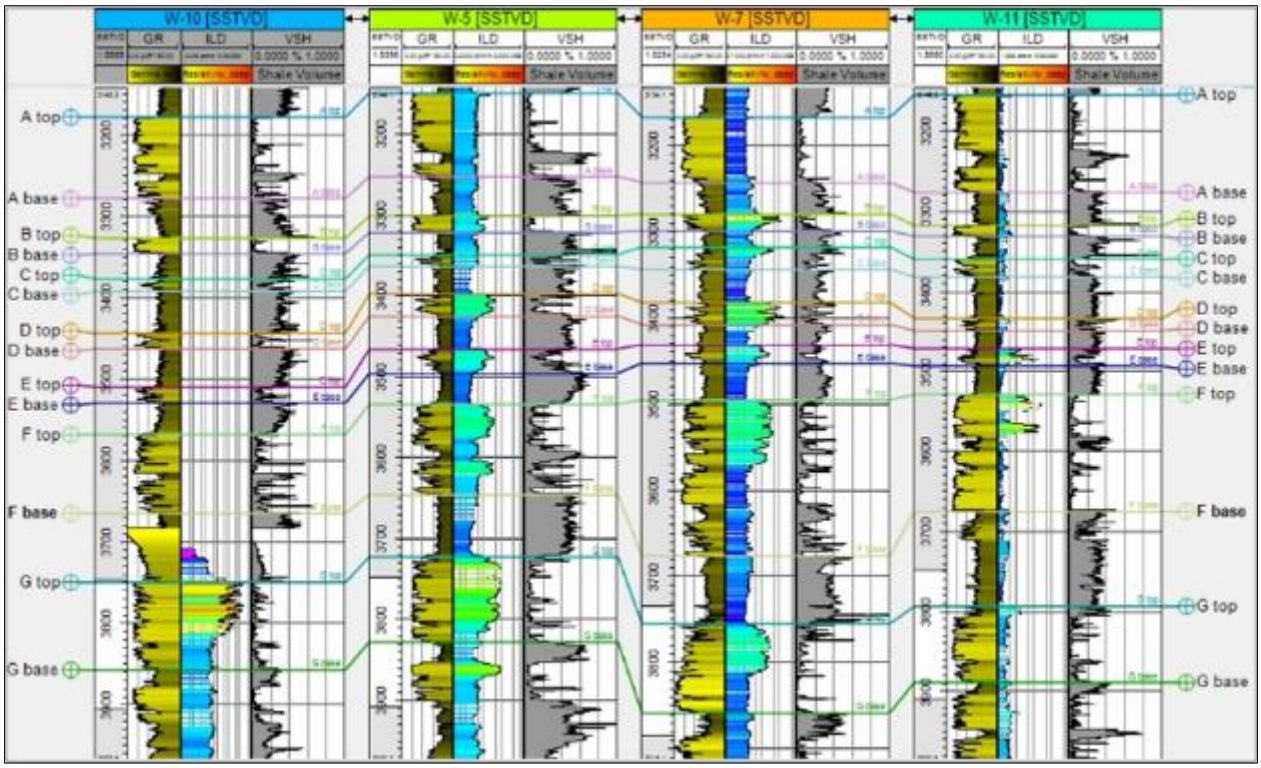

Figure 5 Well section showing shale volume estimated across the field

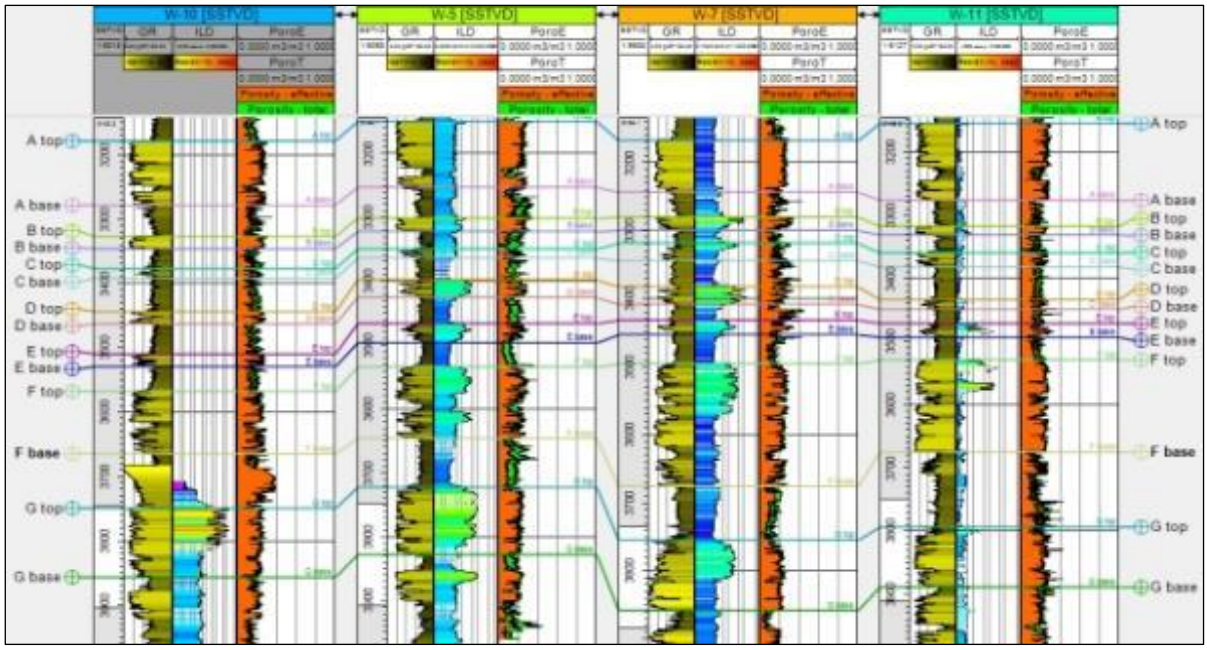

Figure 6 Well section showing Total and effective porosity estimated across the field

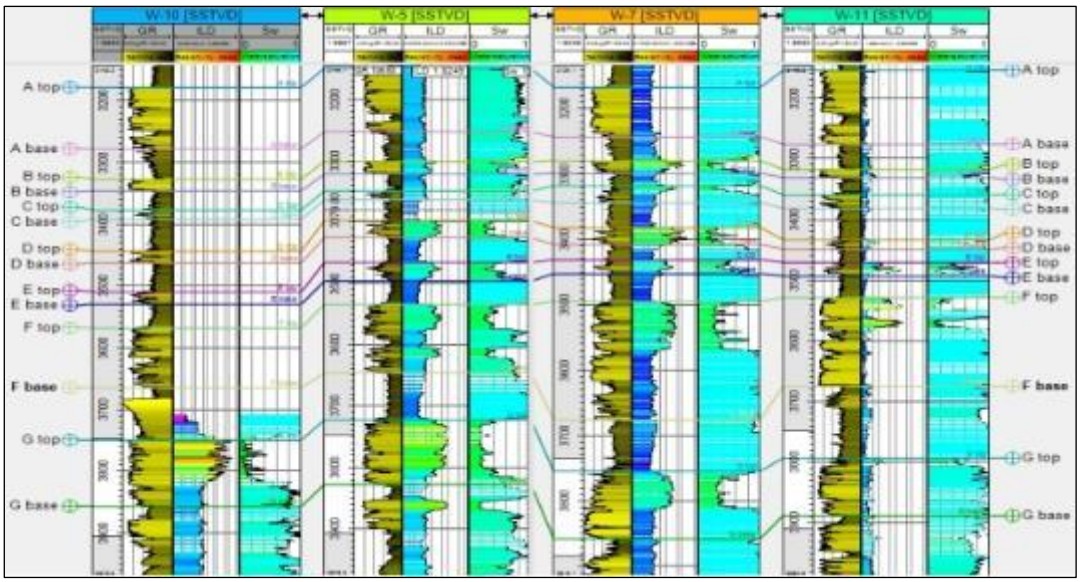

Figure 7 Well section showing water saturation estimated across the field

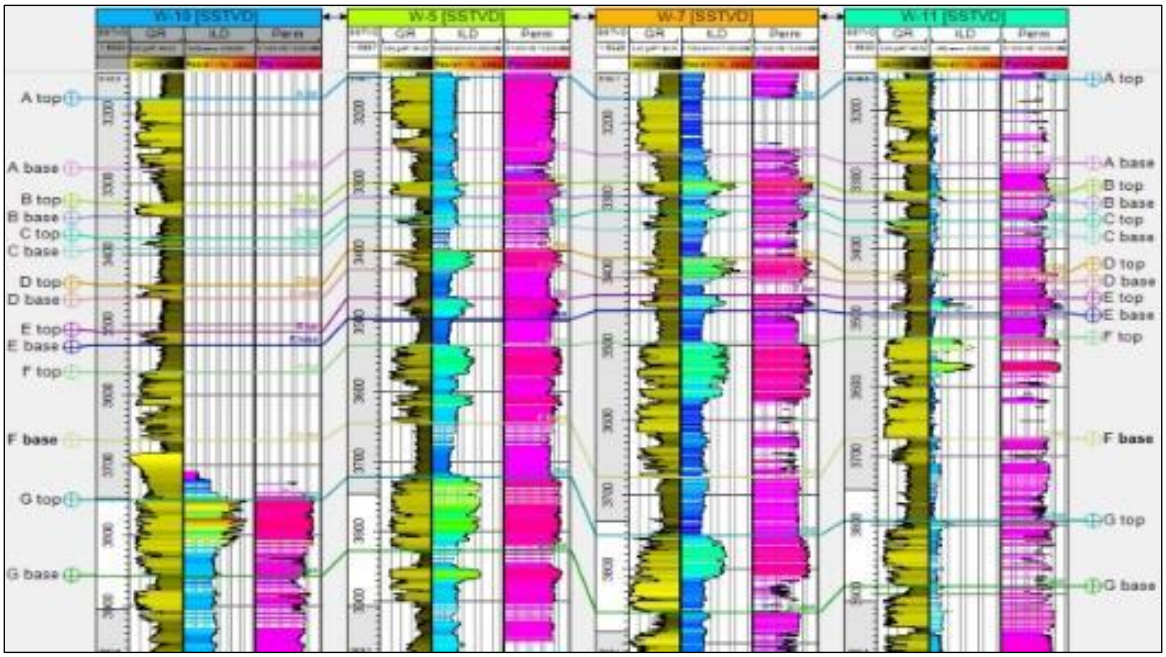

Figure 8 Well section showing permeability estimated across the field

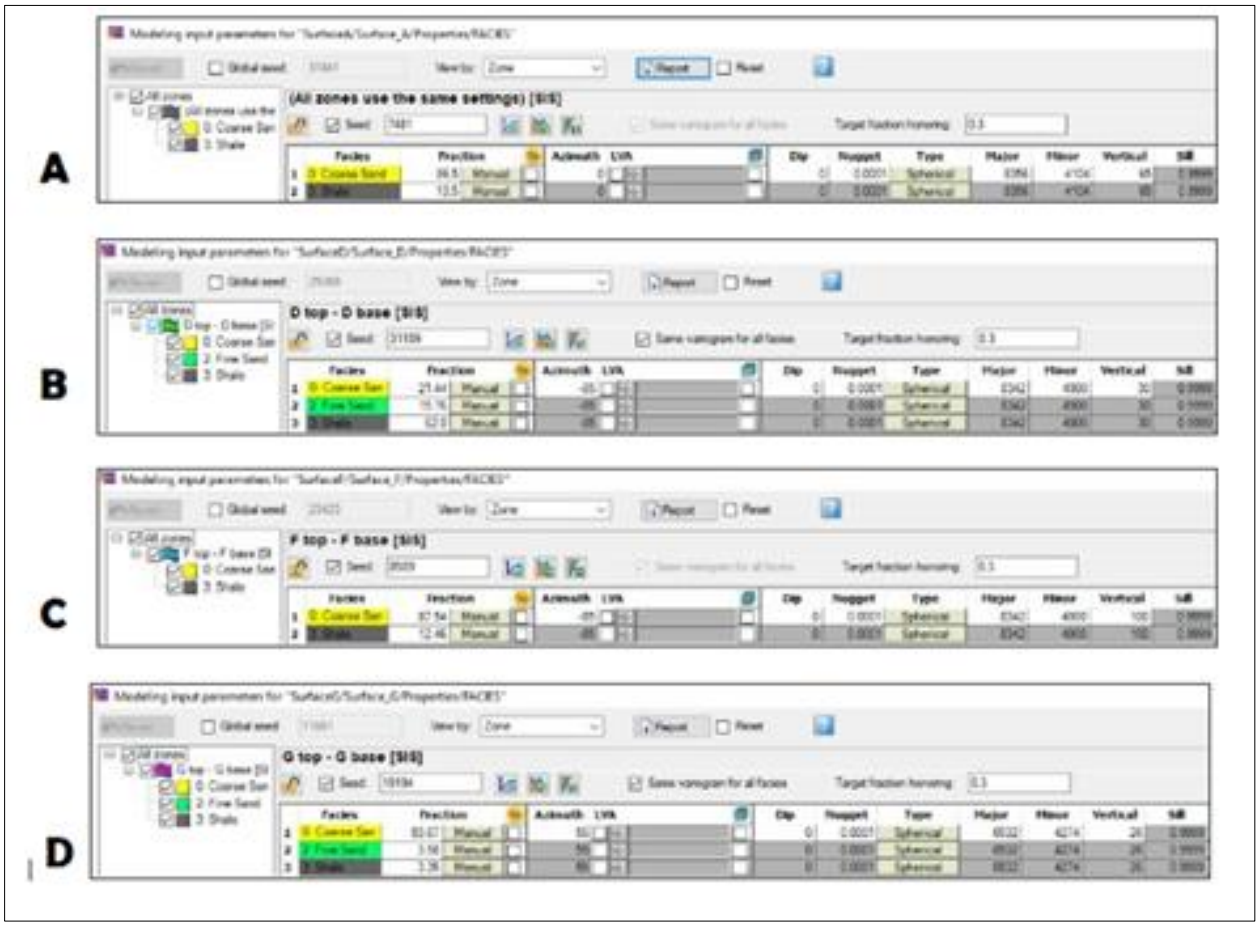

Figure 9 Facies modelling input parameters for (a) Surface A, (b) Surface D, (c) Surface F, (d) Surface G

Figure 10 Facies model generated for (a) Surface A, (b) Surface D

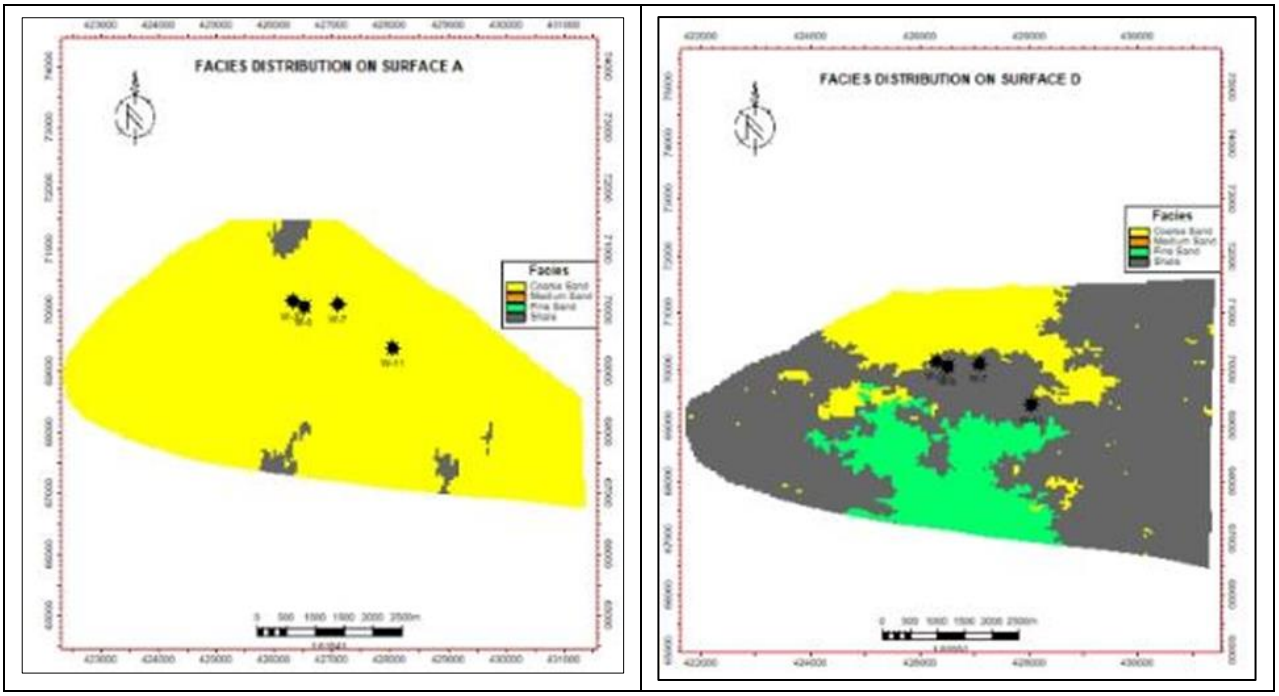

Figure 11 Facies model generated for (c) Surface F, (d) Surface G

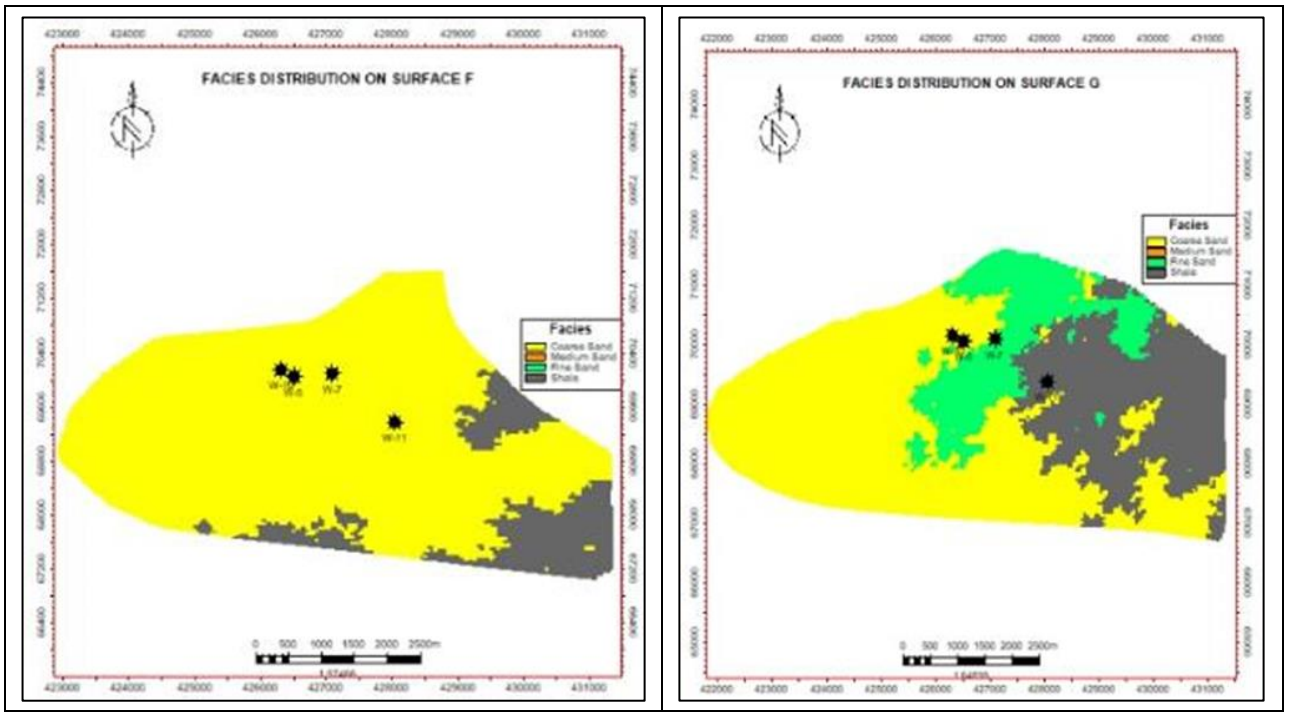

Table 6 Results for map-based (deterministic) hydrocarbon volume estimation for selected reservoir

Zones	HC Area[m^2]	Bulk volume[m^3]	STOIIP[STB]
Reservoir A	457,654.07	6,130,629.00	740.90 MM
Reservoir D	8,287,253.61	124,165,454.00	37.38 MM
Reservoir F	8,774,889.00	668,768,737.00	197.93 MM
Reservoir G	6,325,933.05	173,108,740.00	85.88 MM

Table 7 Results for model based (stochastic) hydrocarbon volume estimation for selected reservoir

	STOIIP (STB)	HCPV (rm^3)	Pore volume (rm^3)	Net Volume (m^3)	Bulk volume (m^3)
P value	Reservoir A				
P10	423.257 M	85,461.62	1,279,821.60	5,169,271.89	5,265,402.38
P50	512.247 M	103,429.95	1,290,361.69	5,239,794.06	5,265,402.38
P90	679.902 M	137,281.72	1,308,065.30	5,243,328.71	5,265,402.38
	Reservoir D				
P10	38.07 MM	7,687,353.28	12,611,353.92	71,495,055.68	119,078,068.63
P50	41.37 MM	8,354,011.50	14,530,072.39	79,019,347.66	119,078,068.63
P90	48.32 MM	9,756,888.67	15,745,619.43	83,885,965.70	119,078,068.63
	Reservoir F				
P10	159.16 MM	32,136,540.51	112,884,730.04	530,817,656.61	650,886,155.52
P50	210.00 MM	42,403,156.16	118,163,766.40	563,370,344.63	650,886,155.52
P90	273.21 MM	55,164,733.25	119,187,518.98	575,570,779.89	650,886,155.52
	Reservoir G				
P10	61.09 MM	12,334,535.39	29,674,521.95	153,950,139.04	187,034,441.94
P50	65.04 MM	13,132,506.85	30,300,297.00	156,382,757.50	187,034,441.94
P90	79.26 MM	16,004,528.06	30,571,135.28	157,076,056.33	187,034,441.94

6. Results of Petrophysical Evaluation

The results of petrophysical evaluation are presented in Tables 4.1-4.4 and Figures 4.2-4.5. These petrophysical results are summarized in Table 4.5 and Figures 4.6-4.8 respectively.

6.1. Gross Thickness

Across the field, the gross thickness of the reservoir sand bodies exhibits variability from one well to another. However, the average gross thickness of the reservoir sands in each sand body is:

- Sand A: 105.25m
- Sand B: 16.50m
- Sand C: 13.25m
- Sand D: 20.00m

- Sand E: 23.75m
- Sand F: 116.00m
- Sand G: 92.75m

This data reveals that Sand A, F, and G have the most significant gross thickness across the field, indicating potential for substantial hydrocarbon accumulation. Notably, the gross thickness of the reservoir intervals is sufficient to support economic quantities of hydrocarbon accumulation, making these sand bodies promising targets for exploration and production. The variability in gross thickness across the field highlights the complexity of the reservoir architecture, emphasizing the need for detailed characterization and modeling to optimize hydrocarbon recovery.

6.2. Shale Volume

The average shale volume thicknesses for each sand body are:

- Sand A: 16%
- Sand B: 8%
- Sand C: 23%
- Sand D: 25%
- Sand E: 25%
- Sand F: 17%
- Sand G: 9%

These values indicate the proportion of shale within each sand body, with higher shale volumes corresponding to poorer quality reservoir rock. Fortunately, all the reservoir sands have shale volumes less than 30% of the entire gross thickness, indicating that the reservoir sands are predominantly clean and of good quality. This suggests that the sand bodies have minimal shale content, which is essential for optimal hydrocarbon flow and accumulation. The relatively low shale volumes also imply that the sand bodies have good porosity and permeability, making them suitable for hydrocarbon production. Overall, the low shale content is a positive indicator for the potential productivity of the reservoir.

6.3. Net thickness

The average reservoir net thickness, which represents the producible portion of the reservoir sand, varies across the different sand bodies:

- Sand A: 88.52m
- Sand B: 15.24m
- Sand C: 10.49m
- Sand D: 14.75m
- Sand E: 17.54m
- Sand F: 97.20m
- Sand G: 84.27m

These results indicate that most of the reservoirs have sufficient thickness available for hydrocarbon accumulation, suggesting a high potential for hydrocarbon production. Furthermore, the Net to Gross ratio (in %), which represents the proportion of clean sand available for hydrocarbon accumulation, is:

- Sand A: 83.88%
- Sand B: 92.50%
- Sand C: 77.25%
- Sand D: 75.00%
- Sand E: 75.50%
- Sand F: 83.25%
- Sand G: 90.75%

Notably, at all reservoir intervals, over 70% of the entire gross thickness is available as clean sand for hydrocarbon accumulation, indicating a high degree of reservoir quality and potential productivity. This suggests that the sand bodies have minimal shale content and are predominantly composed of clean sand, making them suitable for hydrocarbon

production. The high Net to Gross ratio also implies that the reservoirs have good porosity and permeability, further enhancing their potential for hydrocarbon accumulation and production.

6.4. Porosity

The average total porosity in Sand A, Sand B, Sand C, Sand D, Sand E, Sand F and Sand G are 0.25, 0.25, 0.20, 0.24, 0.22, 0.23 and 0.23 respectively. Also, average effective porosity recorded from empirical models are 0.21, 0.24, 0.16, 0.18, 0.17, 0.20 and 0.21 in Sand A, Sand B, Sand C, Sand D, Sand E, Sand F and Sand G. Effective porosity is porosity responsible for hydrocarbon production. Rider (1986) classified porosity as follows; <5% (negligible), 5-10% (poor), >10-20% (good), >20-30% (very good), >30 (excellent). Based on Rider's classification, total porosity recorded in this study is classed as very good while effective porosity is classed as good to excellent.

6.5. Permeability

The average permeability results recorded in this study are 381.74, 937.62, 373.96, 869.88, 933.56, 745.81 and 967.64 mD in Sand A, Sand B, Sand C, Sand D, Sand E, Sand F and Sand G reservoir intervals. Again, Rider (1986) classified reservoir quality based on permeability as follows; < 10mD (poor to fair), >10-50 mD (moderate), >50-250 mD (Good), >250-1000 mD (very good) and >1000 mD (excellent). Based on Rider's classification, the reservoirs are classed as having very good quality.

6.6. Fluid type

Sand A reservoir which has the largest thickness is completely saturated with water in well W-7 and W-11. Only W-5 well has a small oil column (3m thick) capping a huge reservoir of brine. W-10 well does not have resistivity logs for determining fluid type in Sand A, Sand B, Sand C, Sand D, Sand E and Sand F. Reservoir sand B is completely water saturated in W-11 and completed oil saturated in W-5 well. Sand C is completely water saturated in well W-5 and W-11, and oil and water saturated in W-7 well. Reservoir sand D, E, F, and G all contain oil at the different reservoir intervals in all wells.

6.7. Water saturation

Average water saturation in reservoir sand A, B, C, D, E, F, and G are 0.86, 0.70, 0.99, 0.55, 0.46, 0.64 and 0.47, with an equivalent oil saturation of 0.14, 0.30, 0.01, 0.45, 0.54, 0.36 and 0.53 respectively. These results show that the deeper reservoir intervals are more hydrocarbon bearing than the shallower reservoir intervals.

7. Conclusion

This study utilized seismic data and well logs for building facies and petrophysical logs for "Tanko field" in the onshore Niger Delta. This study recognized four lithofacies based on gamma ray log which included; coarse grained sand facies, medium grained sand facies, fine grained sand facies and shale facies. The facies were used to determine the environment of deposition in seven reservoir intervals (sand A to sand G) correlated across four wells. Five environments of deposition were inferred and included; fluvial channel, channel fill, upper shoreface, tidal channels and shales.

Petrophysical evaluation of all the identified reservoir intervals revealed that their gross thicknesses are sufficient for hydrocarbon accumulation in economic quantities. Shale volume is below 30% in all the reservoirs. The total porosity recorded are very good (>20%) while effective porosity is good to excellent (>15%) for the various reservoir intervals. Permeability is classed as very good for all reservoir intervals (> 380.00mD). Water saturation varied but generally decreases with depth.

Facies models generated were used to constrain the petrophysical properties distribution across the reservoir for hydrocarbon volume estimation. Petrophysical models generated included shale volume, effective porosity, permeability and water saturation models. The facies models analysis revealed that both good, moderate and poor sand quality are found in the various reservoir intervals (A, D, F, G) which support the properties from petrophysics in terms of shale volume, porosity and permeability. All the reservoir intervals are hydrocarbon bearing as revealed from the oil water contact model.

Recommendation

Based on this study, the following recommendations were proffered;

- Each well has a specific area which it can drain which is called the drainage area, hence, more wells should be drilled into the identified structure in order to adequately drain the reserves.
- The dynamic simulator should utilize these models as a basis for simulating production plans.
- As new wells are drilled into the structure, the models generated from this study must be re-validated to include the new obtained information before any further production decisions are to be made.

Compliance with ethical standards

Disclosure of conflict of interest

No conflict of interest to be disclosed.

References

[1] Adegoke, O.S., Oyebamiji, A.S., Edet, J.J., Osterloff, P.L., Ulu, O.K. (2017). Cenozoic foraminifera and calcareous nannofossil biostratigraphy of the Niger Delta. Cathleen Sether, United States, 570 pp.

[2] Adeoti, L., Onyekachi, N., Olatinsu, O., Fatoba, J., Bello, M. (2014). Static reservoir modeling using well log and 3-D seismic data in a KN Field, Offshore Niger Delta, Nigeria. International Journal of Geosciences, 5, 93-106.

[3] Adesida, A., and Ehirim, B.O. (1988). Cenozoic Niger Delta: A guide to its lithosedimentary analysis. SPDC Exploration note 88.002 (Ref: on-shore wells). pp. 1–10.

[4] Adiela, U.P., Jackson, C.A., Oyewole, A.M. (2017). Petroleum Prospectivity and Depositional Model of F-Reservoir Sands, Niger Delta, Nigeria. Mediterranean Journal of Basic and Applied Sciences, 1(1): 270-279.

[5] Adikwu, S.O., Oluoma, C.F., Oleson, J., Obaje, E.C. (2017). 3-D Seismic Interpretation and Petrophysical Analysis of "Olu Field" Onshore Niger Delta. International Journal of Geophysics and Geochemistry, 4(6): 73-82.

[6] Aigbadon, G.O., Okoro, A.U., Una, C.O., Ocheli A. (2017). Depositional facies model and reservoir characterization of Usani field 1, Niger delta basin, Nigeria. International Journal of Advanced Geosciences, 5(2): 57-68.

[7] Ailin J., Dongbo and Chengye, J. (2014). Advances and Challenges of Reservoir Characterization: A Review of The Current State of the Art. Intech Online Publisher, 51000 Rijeka, Croatia.

[8] Ajibola, O.O. (2004). Sequence Stratigraphy of the Niger Delta, Delta Field, Offshore Nigeria. An unpublished dissertation submitted to the School of Graduate Studies of Texas A&M University, United States of America.

[9] Avbovbo, A. A. (1978). Tertiary Lithostratigraphy of the Niger Delta. American Association of Petroleum Geologists Bulletin. 62(2): 295 – 306.

[10] Burke, K. (1972). Longshore drift, submarine canyons, and submarine fans in development of Niger Delta: American Association of Petroleum Geologists, 56, 1975-1983.

[11] Cannon, S. (2018). Reservoir Modelling: A Practical Guide. John Wiley and Sons, Inc., 111 River Street, Hoboken, NJ 07030, USA. ISBN: 9781119313434.

[12] Department of Petroleum Resources (DPR). (2005). Nigerian Department of Petroleum Resources (DPR) 2005 bid round report.

[13] Doust, H. and Omatsola, E. (1990). Niger Delta, In: Edwards, J.D. and Santogrossi, P.A. (eds.), Divergent/passive Margin Basins, AAPG Memoir 48, 239-248.

[14] Dresser Atlas (1979). Log Interpretation Charts, Dresser Industries Inc., Houston, Texas: p.107

[15] Ejedawe, J.E. (1981). Patterns of incidence of oil reserves in Niger Delta Basin: American Association of Petroleum Geologists, 65, 1574-1585.

[16] Ejeke, C.F. Anakwuba, E.E., Preye, I.T. Kakayor, O.G., and Uyouko, I.E. (2017). Evaluation of reservoir compartmentalization and property trends using static modelling and sequence stratigraphy. J. Petrol. Explor. Prod. Technol., 7:361–377.

[17] Emery, D., Myers, K.J. (1996). Sequence stratigraphy. Blackwell, Oxford, pp.29.

[18] Jong-Se, L. (2005). Reservoir Properties Determination Using Fuzzy Logic and Neural Networks from Well Data in Offshore Korea. Journal of Petroleum Science and Engineering 49(3): 182-192.

[19] Kogbe, C.A. (1989). The Cretaceous Paleocene Sediments of Southern Nigeria. In C.A. Kogbe (Ed.), Geology of Nigeria. Jos: Rock View Ltd., 320–325.

[20] Kulke, H. (1995). Nigeria, in, Kulke, H., ed., Regional Petroleum Geology of the World. Part II: Africa, America, Australia and Antarctica: Berlin, Gebrüder Borntraeger, 143-172.

[21] Larionov, V. (1969). Borehole Radiometry: Moscow, U.S.S.R., Nedra.

[22] Lehner, P., and De Ruiter, P.A.C. (1977). Structural history of Atlantic Margin of Africa: American Association of Petroleum Geologists Bulletin, 61, 961-981.

[23] Olade, M.A. (1975). Evolution of Nigeria's Benue Trough (Aulacogen): A Tectonic Model, Geological Magazine, 112, 6, 575-583.

[24] Ogbe, O. B. (2020). Sequence stratigraphic controls on reservoir characterization and architectural analysis: a case study of Tovo field, coastal swamp depobelt, Niger Delta Basin, Nigeria.

[25] Ogbe, O. B. (2021). Depositional facies, sequence stratigraphy and reservoir potential of the Eocene Nanka Formation of the Ameki Group in Agu-Awka and Umunya, southeast Nigeria.

[26] Owolabi, O.O., Longjohn, T.F., Ajienka J.A. (1994). An empirical expression for permeability in unconsolidated sands of eastern Niger Delta: J. Pet. Geol. 17(1): 111-116.

[27] Rider, M.H. (1986). The Geological Interpretation of Well Logs. 2nd Ed. Whittles Publishing: Caithness.

[28] Ringrose, P.S. and Bentley, M. (2015). Reservoir Model Design, Springer Science, Business, Dordrecht, Netherlands.

[29] Schlumberger (1974). Log Interpretation Charts, Schlumberger Educational Services, New York, 83p.

[30] Short, K.C., Stauble, A.J. (1967). Outline of Geology of Niger Delta. Am. Assoc. Petr. Geol. Bull., 51(5): 761–779.